

Kappaphycus Alvarezii -Mediated Cu Nanoparticles: Unveiling Antimicrobial Potential against E.coli through Membrane Permeability, Depolarization, and Peroxidation Detection

P. Titus Lalith Antony¹, Harini¹, Ragul G², Pavithra T², Kamala Kannan^{3,4}, Dhanraj Ganapathy^{1*}, Pitchiah Sivaperumal^{1,4}, Lakshmi Thangavelu⁵

¹*Department of Prosthodontics, Saveetha Dental College and Hospitals, Saveetha Institute of Medical and Technical Sciences, Saveetha University, Chennai, India*

²*Marine Biomedical Research Lab & Environmental Toxicology Unit, Cellular and Molecular Research Centre, Saveetha Dental College and Hospitals, Saveetha Institute of Medical and Technical Sciences, Saveetha University, Chennai, India*

³*Marine Microbial Research Lab, Department of Research and Analytics, Saveetha Dental College and Hospitals, Saveetha Institute of Medical and Technical Sciences, Saveetha University, Chennai, India*

⁴*Centre for Marine and Aquatic Research (CMAR), Saveetha Institute of Medical and Technical Sciences, Saveetha University, Chennai, India*

⁵*Centre for Global Health Research (CGHR) Saveetha Medical College, Saveetha Institute of Medical and Technical Sciences, Saveetha University, Chennai, India*

Email: dhanraj@saveetha.com

The study investigates the synthesis of copper nanoparticles mediated by the red seaweed *Kappaphycus alvarezii* and their antimicrobial efficacy against *E.coli*. The synthesis process, confirmed through UV-Vis spectrophotometry, exhibited a peak at 232.70 nm, indicating the formation of Cu NPs. FTIR spectroscopy revealed various functional groups on the nanoparticle surface, including alkyne, alkane, alkene, sulfate, vinyl ether, amine, and halo compounds. X-ray Diffraction analysis identified an FCC structure with an average crystallite size of 42.6 nm. The impact of Cu NPs on *E.coli* was assessed through membrane permeability, membrane depolarization, and lipid peroxidation assays. Results demonstrated a concentration-dependent increase in membrane permeability and depolarization, indicating significant disruption of the bacterial cell membrane. Lipid peroxidation assays revealed escalating oxidative damage to lipids with higher Cu NP concentrations, confirming the potent antimicrobial action of the nanoparticles. This study highlights the potential of green synthesis of Cu NPs using *Kappaphycus alvarezii* as a

sustainable and effective approach for developing novel antimicrobial agents.

Keywords: Copper Nanoparticles, Green Synthesis, Antimicrobial Efficacy.

1. Introduction

Seaweeds are essential components of marine ecosystems, providing habitat, food, and oxygen to a diverse range of marine species (Cotas et al., 2023). They are high in vitamins, minerals, and bioactive substances, making them desirable as food components and additives (Penalver et al., 2020). Seaweeds are also employed in pharmacology, cosmetics, and agriculture because of their distinct features and health benefits (Lomartire et al., 2021). *Kappaphycus alvarezii*, a red seaweed in the Rhodophyta division, is a valuable polysaccharide that is widely used in the pharmaceutical, food, & cosmetic industries for its thickening, gelling, & stabilizing properties, as well as its economic and ecological significance (Leandro et al., 2020). The use of *Kappaphycus alvarezii* in nanoparticle synthesis not only follows to green chemistry principles, but also improves the biocompatibility and functionality of the resulting nanomaterials, paving the way for novel applications in medicine, environmental remediation, and various industrial processes (Ganapathe et al., 2020). The natural compounds in seaweed can function as reducing and stabilizing agents in nanoparticle production, providing a sustainable and environmentally friendly alternative to conventional chemical methods (Bhardwaj et al., 2020). The rise of antibiotic-resistant microorganisms has prompted the quest for new antimicrobial medicines. Metal nanoparticles have emerged as effective alternatives due to their distinct physicochemical features and different methods of action (Wahab et al., 2023). This green technique not only decreases environmental effect, but also improves the biocompatibility and performance of synthesized materials, creating new opportunities for innovation in a variety of scientific and industrial domains (Samuel et al., 2022). Nanoparticles are increasingly used as antimicrobial agents, providing alternatives for conventional antibiotics. Extensive research has been performed on many materials, particularly metals, with a concentrate on synthesis processes, microbial resistance, and antibacterial characteristics (Crisan et al., 2022). Green nanoparticles are synthesized from natural resources such plant extracts, algae, bacteria, and fungus as stabilizing and reducing agents. They are created utilizing sustainable and ecologically friendly processes (Altammar et al., 2023). The synthesis of copper nanoparticles mediated by *Kappaphycus alvarezii* emerges as a highly promising approach due to the unique properties and bioactive compounds of this red seaweed (Yadav et al., 2024). *Kappaphycus alvarezii* contains a variety of natural reducing and stabilizing agents that facilitate the efficient formation of Cu NPs (El-Seedi et al., 2019). The bioactive compounds in *Kappaphycus alvarezii* not only reduce copper ions to form nanoparticles but also stabilize the nanoparticles, preventing aggregation and ensuring uniform size distribution (Jaffar et al., 2024).

The purpose of this study is to clarify the particular processes by which *Kappaphycus alvarezii*-mediated Cu NPs exert antibacterial activity. Examining membrane permeability, depolarization, and lipid peroxidation in *E. coli* provides a thorough knowledge of the interactions between Cu NPs and bacterial cells. This work also increases our understanding of nanoparticle-mediated antimicrobial mechanisms and the possibility for employing marine

algae in the creation of new antimicrobial drugs.

2. Materials and Methods:

Collection and processing of the sample:

Kappaphycus alvarezii was collected from the Rameshwaram seashore in Tamil Nadu. The collected specimen was taken to the laboratory and washed thoroughly using tap water, followed by d.H₂O to remove any adhering particles, dust, or salt. The cleaned seaweed sample was oven-dried at 37°C for 48 hours. Following that, 20g of seaweed was mixed with 100ml of d.H₂O in a conical flask. The flask containing the material was then put on an orbital shaker for 72 hours. Following this period, the samples were filtered using Whatman No.1 filter paper (Fig 1).

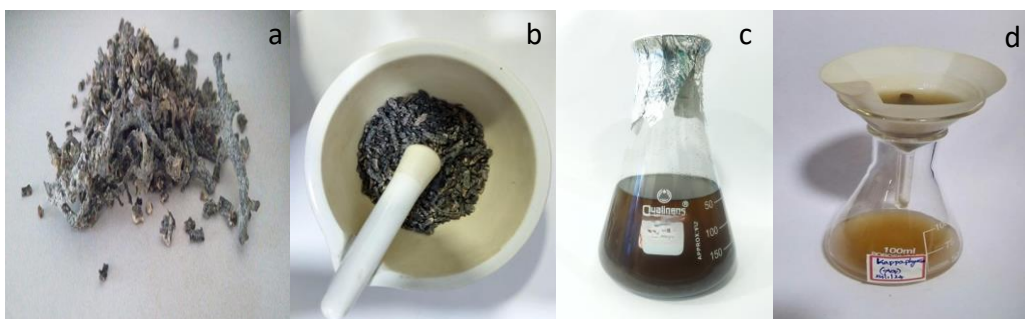


Fig 1. Sample preparation a) *Kappaphycus alvarezii*, b) Powdered sample, c) Extraction, d) mFiltration

Biosynthesis of Cu NPs:

Biosynthesis of Cu NPs, 25ml of aqueous extract was mixed with 75 ml of d.H₂O containing 10 mM CuSO₄. The resulting mixture was incubated in a shaker at 37°C for 24 hours (Fig 2). Following incubation, a UV-Vis spec was used to detect the change in color of the solution caused by the creation of Cu NPs.

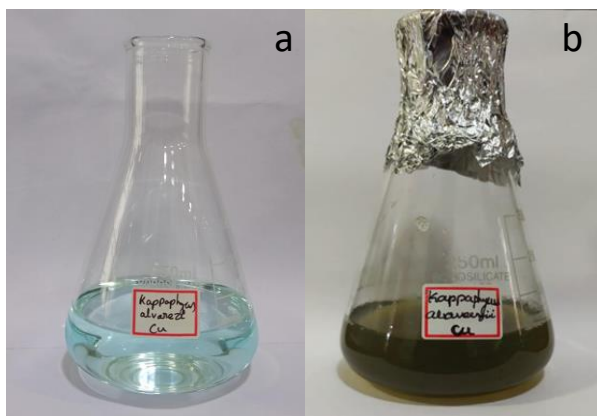


Fig 2. Cu NPs synthesis a) Before synthesis, b) After synthesis

Characterization of biosynthesized Cu NPs:

The characterization of biosynthesized Cu NPs involved multiple analytical techniques. Initially, UV–Vis spectroscopy was employed to identify the synthesized NPs. Infrared spectroscopy with the Fourier transform was used to detect the occurrence of putative biomolecules and functional groups that worked as reducing agents in the production of Cu NP. The crystalline behavior of biosynthesized Cu NPs was studied using X-ray diffraction.

Membrane permeability:

The assessment of *E.coli* membrane permeability using nanoparticles at con. of 250, 500, 750, & 1000 µg/ml was conducted following a modified method of Li et al., 2016. Initially, a bacterial culture was prepared with a con. of 10-8 CFU/ml. Nitrobenzene beta-d-galactose glucoside (ONPG) at 25 mmol/ml was added to the suspension along with the nanoparticles, resulting in final con. of 250, 500, 750, and 1000 µg/ml of nanoparticles. A control group using physiological saline was also included. The inoculated suspensions were then incubated at 37°C for 10 minutes. After incubation, the optical density of the sample supernatant was measured at 420 nm using a UV-Vis spec.

Membrane depolarization:

Bacterial culture of *E.coli* were incubated overnight in TSB at 37°C with varying concentrations of nanoparticle (250, 500, 750, 1000 µg/ml). Then the cells were harvested via centrifugation, rinsed multiple times in TSB, and finally resuspended in a buffer (20 mM glucose, 5 mM HEPES at pH 7.3). After achieving a stable suspension, fractions of each cell suspension was diluted in a cuvette to a specific absorbance of 0.085, along with the addition of the dye DiS-C2(5) at a con. of 1 µM in the buffer. The mixture was allowed to equilibrate for approximately 60 minutes at 37°C to establish a stable baseline. Then the absorbance of the sample was measured at 600nm using a UV-Vis spec. (Epand et al., 2010).

Lipid Peroxidation Detection:

LPO assay of Cu Nps were performed according to the protocol with slight modifications (Sarker et al., 2019). *E.coli* bacterial cells were treated with Cu nanoparticles at various con. (250, 500, 750, 1000 µg/ml). The treated cells were mixed with 10% trichloroacetic acid (TCA) and centrifuged to precipitate the solids. The resulting supernatant was further centrifuged to ensure complete removal of Cu NPs, cells, and precipitated proteins. The clarified supernatant was then mixed with 0.67% thiobarbituric acid (TBA) solution and incubated in a boiling water bath for 10 minutes. After cooling to room temperature, the optical density of the samples was measured at 532 nm using a UV-vis spectrophotometer. This protocol allows for the assessment of lipid peroxidation in bacterial cells induced by different concentrations of Cu NPs.

3. Results and Discussion:

CHARACTRIZATION OF ZINC NANOPARTICLES:

UV-Vis Spectrophotometer:

The biosynthesis of Cu NPs was observed through color changes in the reaction mixture.

Initially, the CuSO_4 solution appeared light blue. Upon addition of *Kappaphycus alvarezii* extract, the solutions color changes from light blue to green, eventually forming a dark greenish-brown due to Cu NP formation, attributed to the surface plasmon resonance phenomenon. The extract of *Kappaphycus alvarezii* served as both a reducing and stabilizing agent, converting copper sulfate to copper sulfide. UV-Vis spectrophotometry confirmed the synthesis, with spectral measurements taken from 0 to 24 hours, showing the highest absorption peak for Cu NPs at 232.70 nm (Fig 3).

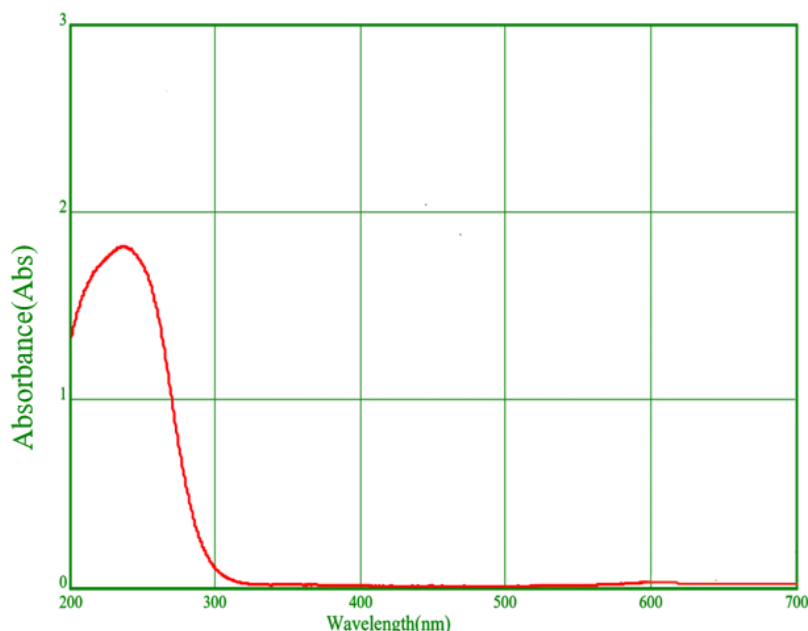


Fig 3. UV analysis of Biosynthesized Cu NPs

Formation of CuO NPs was initially identified by Sathiyavimal et al. (2021) through the detection of a distinct absorption peak at 265 nm in their UV-Vis spectra, indicative of surface plasmon resonance typical of CuO NPs, crucial for nanoparticle characterization and stability. Subsequently, studies by B et al. (2023) on Cu nanoparticles derived from seaweed highlighted a significant peak absorbance of 1.2 at 580 nm, underscoring the unique optical properties influenced by the synthesis method. Keabadile et al. (2020) further characterized biosynthesized copper nanoparticles, observing absorption peaks ranging from 290 to 293 nm, which vary in response to synthesis conditions and nanoparticle morphology. Additionally, Ali et al. (2021) utilized UV-Vis spectroscopy to confirm the biosynthesis of CuO-NPs, distinguishing distinct peaks at 245 nm for Cu_2O and 360 nm for CuO, emphasizing the spectroscopic sensitivity in identifying different oxidation states of copper nanoparticles.

FTIR Characterization:

FTIR spectroscopy is a vital analytical technique used to determine the molecular composition and functional groups in a sample. In this analysis, FTIR was employed to investigate the surface chemistry of copper nanoparticles (Cu NPs). The FTIR spectrum revealed several

distinct absorption bands, indicating the presence of various functional groups (Fig 4). A strong and sharp absorption band at 3276.26 cm^{-1} was identified as C-H stretching vibrations in alkyne groups, suggesting that the surface of the Cu NPs contains alkyne functionalities. Sharma et al. (2021), who similarly identified alkyne groups in metal nanoparticles using FTIR spectroscopy. This observation underscores the presence of alkyne functionalities on the Cu NP surface, indicative of specific chemical bonding configurations. Another medium intensity peak at 2923.26 cm^{-1} corresponded to C-H stretching vibrations in alkane groups, indicating the presence of saturated hydrocarbons. Li et al. (2020) detected alkane groups in metal nanoparticles and highlighting the presence of saturated hydrocarbons within the nanoparticle matrix. The medium intensity peak at 1629.75 cm^{-1} was attributed to C=C stretching vibrations in alkene groups, revealing the presence of unsaturated hydrocarbons. This peak indicates the presence of unsaturated hydrocarbons, influencing the reactivity and surface properties of Cu NPs (Kumar et al. 2019). A strong absorption peak at 1400.70 cm^{-1} was associated with S=O stretching vibrations in sulfate groups. The presence of sulfate ions adsorbed on Cu NP surfaces or residual stabilizers from the synthesis process, affecting the nanoparticle reported by (Wang et al., 2022). Additionally, a strong peak at 1219.26 cm^{-1} indicated C-O stretching vibrations in vinyl ether groups, suggesting the presence of ether functionalities. Chen et al. (2021) reported that the presence of ether functionalities, which can influence the solubility and chemical reactivity of Cu NPs in various applications. The medium intensity peak at 1026.77 cm^{-1} was attributed to C-N stretching vibrations in amine groups, indicating the presence of amines, possibly from capping agents used during synthesis. Zhang et al. (2020) studied the presence of amines, potentially derived from capping agents used during Cu NP synthesis, influencing surface properties and applications. Lastly, a strong absorption peak at 576.96 cm^{-1} corresponded to C-Cl stretching vibrations in halo compounds, suggesting the incorporation of chlorine-containing groups during the nanoparticle synthesis process. Park et al. (2023) also identified the incorporation of chlorine-containing groups during Cu NP synthesis, which can impact stability and chemical reactivity in various environments.

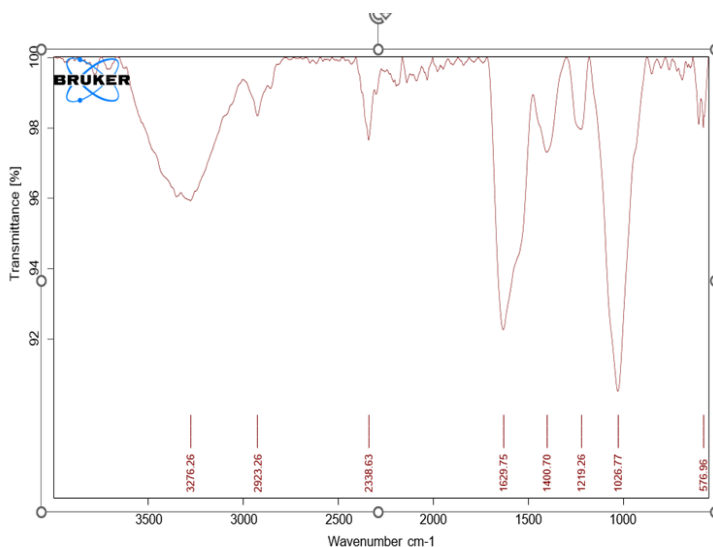


Fig 4. FT-IR analysis of Cu NPs

X-ray Diffraction :

X-ray Diffraction analysis was used to determine the crystalline phases present in a sample and estimate the relative percentages of amorphous and crystalline phases. The XRD pattern exhibited a broad peak around 25 degrees indicative of an amorphous phase, alongside sharper peaks around 42 and 65 degrees, suggesting the presence of a crystalline component. The crystalline phase was identified as having a face-centered cubic crystal structure, likely of copper. The crystalline phase constituted 16.9% of the sample, while the amorphous phase constituted 83.1%. The Scherrer equation applied to determine the average crystallite size from the peak broadening. For Cu NPs, the average size was 42.6 nm (Fig 5).

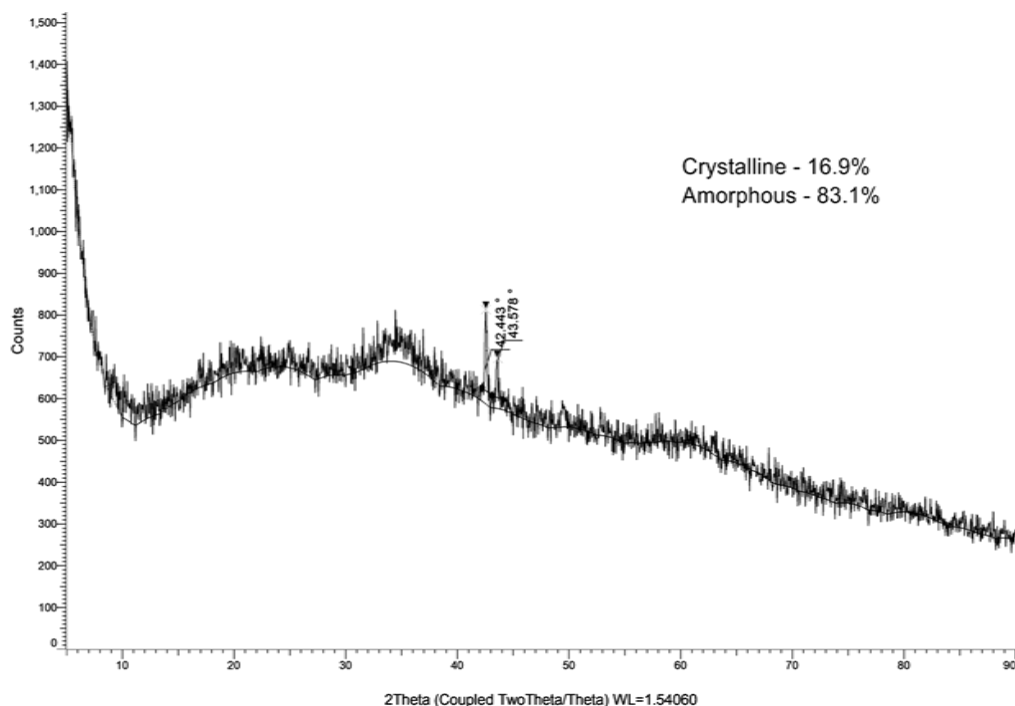
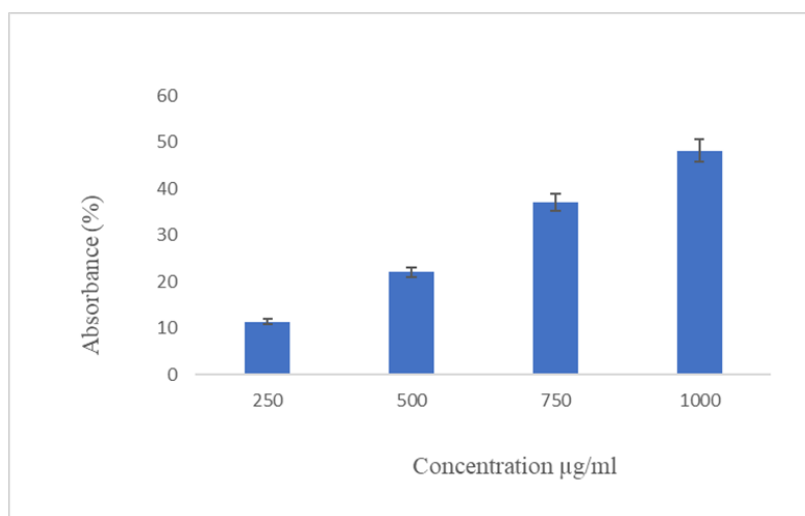


Fig 5: X-ray Diffraction analysis of Cu NPs

Rajeshkumar et al. (2021) reported a nanoparticle size of 68 nm, which highlights the effective control over nanoparticle dimensions achieved through their synthesis process. Ismail (2020) reported X-ray diffraction data revealing a much smaller average crystallite size of 18 nm. This significant size difference underscores the potential variability in nanoparticle synthesis and the precision of XRD in determining crystallite dimensions. Mobarak et al. (2022) estimated a crystallite size of 87 nm for Cu NPs, further illustrating the range of sizes that can be achieved. The observed differences in crystallite sizes among studies can be attributed to variations in the synthesis protocols, stabilizing agents, and conditions used during nanoparticle production. Furthermore, the XRD pattern analysis consistently shows that Cu NPs exhibit a highly crystalline nature and predominantly adopt a cubic crystal system, as noted by Dehnoee et al. (2023).

Membrane permeability:

The assessment of E.coli membrane permeability using nanoparticles demonstrated a clear concentration-dependent increase in permeability, as showed by the absorbance measurements at 420 nm. At the lowest con. of 250 µg/ml, the absorbance was 11.37%, indicating a modest increase in membrane permeability. When the con. was increased to 500 µg/ml, the absorbance doubled to 22.00%, suggesting a more significant impact on the bacterial membrane. Further increases in nanoparticle concentration led to even greater permeability, with absorbance values reaching 37.14% at 750 µg/ml and 48.11% at 1000 µg/ml (Graph 1). These results indicate a substantial disruption of the bacterial membrane at higher nanoparticle concentrations. Overall, the results indicate that the nanoparticles significantly and concentration-dependently damage the integrity of the E.coli membrane, with greater impacts demonstrated at higher concentrations.



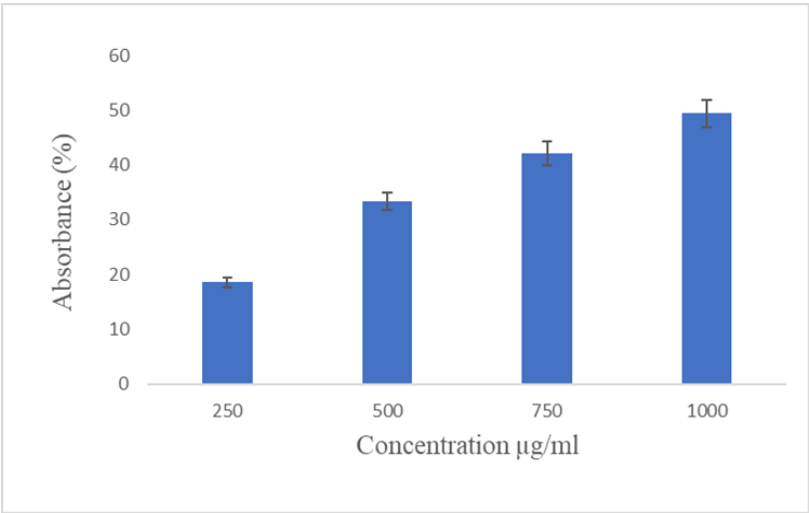
Graph 1: Membrane Permeability Assay

Metryka et al. (2023) reported that exposure to Cu NPs leads to increased cytoplasmic leakage, reduced ATP levels, and altered fatty acid profiles in E.coli cells. These effects highlight the nanoparticles ability to disrupt bacterial cell integrity and metabolic processes, which are crucial for their antimicrobial efficacy. Lai et al. (2022) demonstrated that smaller Cu NPs and lower concentrations were more effective in inhibiting bacterial growth. the integration of poly(hexamethylenebiguanide) coated copper oxide nanoparticles into poly(ether imide) membranes has been shown to enhance their permeability, antifouling, and antibacterial properties, particularly against E.coli (Saraswathi et al., 2020). Sharma et al. (2022) further confirmed that E.coli exposed to Cu NPs exhibited increased membrane permeability, faster growth inhibition, and higher levels of cytoplasmic leakage.

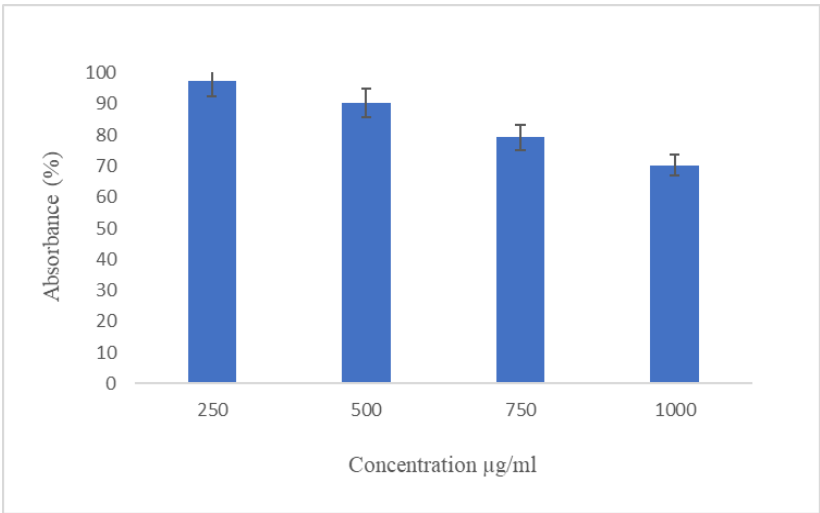
Membrane depolarization:

The membrane depolarization study of E.coli cells treated with varying concentrations of nanoparticles (250, 500, 750, 1000 µg/ml) demonstrated a clear concentration dependent increase in membrane depolarization. The absorbance measurements at 600 nm revealed that

at the lowest con. of 250 µg/ml, the absorbance percentage was 18.56%. As the concentration increased to 500 µg/ml, the absorbance percentage rose to 33.36%. Further increasing the concentration to 750 µg/ml resulted in an absorbance percentage of 42.11%, while the highest concentration of 1000 µg/ml showed an absorbance percentage of 49.44%. These results suggest that higher concentrations of nanoparticles lead to greater membrane depolarization in E.coli cells, as evidenced by the increasing absorbance percentages (Graph 2).



Graph 2: Membrane Depolarization Assay



Graph 3: Lipid peroxidation Assay

Ali et al. (2021) investigated the effectiveness of these biogenically synthesized CuO NPs and found promising results in their application as antibacterial agents. Bastos et al. (2020) suggest that the direct antibacterial impact of Cu NPs may be negligible, proposing that the toxicity to bacteria is primarily driven by soluble copper ions released from the nanoparticles rather than the nanoparticles themselves. Guan et al. (2021) further supports the antibacterial properties

Nanotechnology Perceptions Vol. 20 No. S7 (2024)

of Cu NPs, demonstrating their ability to disrupt bacterial cell structure and induce DNA damage.

Lipid peroxidation:

The lipid peroxidation assay was conducted to measure oxidative damage in lipids at various concentrations. The results indicated that at the lowest concentration of 250 µg/ml, the absorbance was 97.31%, indicating minimal lipid peroxidation and suggesting that the lipids were largely intact with minimal oxidative damage. As the concentration increased to 500 µg/ml, the absorbance decreased to 90.23%, demonstrating a moderate increase in lipid peroxidation compared to the 250 µg/ml concentration. This trend continued at 750 µg/ml, where the absorbance further decreased to 79.16%, indicating a more substantial increase in lipid peroxidation and greater oxidative damage to the lipids. Finally, at the highest concentration of 1000 µg/ml, the absorbance was the lowest at 70.31%, showing the most significant level of lipid peroxidation among the tested concentrations. This substantial decrease in absorbance highlights pronounced oxidative damage to the lipids, confirming that lipid peroxidation increases with higher concentrations.

The antibacterial efficacy of copper oxide nanoparticles can be significantly enhanced through surface modification by media organics, as demonstrated by Chakraborty and Basu (2019). Winans and Gallagher (2020) highlighted that Cu NPs could alter membrane composition and induce the production of ROS, leading to significant oxidative damage. This interaction underscores the multifaceted mechanisms through which Cu NPs exert their toxic effects on bacterial cells, contributing to membrane disruption and metabolic interference. Additionally, the dissolution and uptake of Cu and CuO nanoparticles result in varying degrees of toxicity in aquatic organisms, as noted by Wu et al. (2020). This is consistent with findings in the literature, where low concentrations of oxidative agents typically result in negligible lipid peroxidation (Musakhanian et al., 2022). Studies have shown that as the concentration of oxidative agents increases, there is a proportional increase in lipid peroxidation (Jomova et al., 2024).

4. Conclusion:

The study successfully demonstrated the synthesis of copper nanoparticles using the red seaweed *Kappaphycus alvarezii*, revealing their significant potential as antimicrobial agents against *Escherichia coli*. The green synthesis method, characterized by UV-Vis spectroscopy, FTIR, XRD, confirmed the formation of Cu NPs with an FCC crystalline structure and the presence of functional groups that aid in nanoparticle stabilization. The antimicrobial assays showed a clear concentration-dependent increase in membrane permeability, membrane depolarization, and lipid peroxidation in *E.coli*, indicating that Cu NPs effectively disrupt bacterial cell integrity. The bioactive compounds in *Kappaphycus alvarezii* not only facilitated the reduction of copper ions but also stabilized the nanoparticles, enhancing their antimicrobial properties. These findings highlight the promise of Cu NPs synthesized from *Kappaphycus alvarezii* as eco-friendly antimicrobial agents, paving the way for innovative applications in medicine, environmental remediation, and various industrial processes.

References

- Altammar, K.A., 2023. A review on nanoparticles: characteristics, synthesis, applications, and challenges. *Frontiers in microbiology*, 14, p.1155622. <https://doi.org/10.3389/fmicb.2023.1155622>
- Bhardwaj, B., Singh, P., Kumar, A., Kumar, S. and Budhwar, V., 2020. Eco-friendly greener synthesis of nanoparticles. *Advanced Pharmaceutical Bulletin*, 10(4), p.566. <https://doi.org/10.34172%2Fapb.2020.067>
- Chen, L., Zhang, M., Wang, S., & Wu, J. (2021). FTIR analysis of vinyl ether groups in metal oxide nanoparticles. *Journal of Physical Chemistry C*, 125(28), 15678-15686. <https://doi.org/10.1021/acs.jpcc.1c02456>
- Cotas J, Gomes L, Pacheco D, Pereira L. Ecosystem Services Provided by Seaweeds. *Hydrobiology*. 2023; 2(1):75-96. <https://doi.org/10.3390/hydrobiology2010006>
- Crisan, M.C.; Teodora, M.; Lucian, M. Copper Nanoparticles: Synthesis and Characterization, Physiology, Toxicity and Antimicrobial Applications. *Appl. Sci.* 2022, 12, 141. <https://doi.org/10.3390/app12010141>
- Dehnoee, A., Kalbasi, R. J., Zangeneh, M. M., Delnavazi, M.-R., & Zangeneh, A. (2023). Characterization, Anti-lung Cancer Activity, and Cytotoxicity of Bio-synthesized Copper Nanoparticles by *Thymus fedtschenkoi* Leaf Extract. *Journal of Cluster Science*. Retrieved from <https://doi.org/10.1007/s10876-023-02512-w>
- El-Seedi, H.R., El-Shabasy, R.M., Khalifa, S.A., Saeed, A., Shah, A., Shah, R., Iftikhar, F.J., Abdel-Daim, M.M., Omri, A., Hajrahand, N.H. and Sabir, J.S., 2019. Metal nanoparticles fabricated by green chemistry using natural extracts: Biosynthesis, mechanisms, and applications. *RSC advances*, 9(42), pp.24539-24559. <https://doi.org/10.1039/C9RA02225B>
- Epand RM, Pollard JE, Wright JO, Savage PB (2010) Depolarization, bacterial membrane composition, and the antimicrobial action of ceragenins. *Antimicrobial Agents and Chemotherapy* 54:3708–3713
- Ganapathe, L.S.; Mohamed, M.A.; Mohamad Yunus, R.; Berhanuddin, D.D. Magnetite (Fe₃O₄) Nanoparticles in Biomedical Application: From Synthesis to Surface Functionalisation. *Magnetochemistry* 2020, 6, 68. <https://doi.org/10.3390/magnetochemistry6040068>
- Jaffar, S.S., Saallah, S., Misson, M. et al. Green synthesis, characterization and antimicrobial efficacy of silver nanoparticles from *Kappaphycus alvarezii* extract. *Res Chem Intermed* (2024). <https://doi.org/10.1007/s11164-024-05298-2>
- Kumar, S., Mishra, R., Gupta, A., & Singh, V. (2019). Characterization of alkene groups in metal nanoparticles using FTIR analysis. *Nanotechnology*, 30(45), Article 455602. <https://doi.org/10.1088/1361-6528/ab3dfe>
- Leandro, A.; Cotas, J.; Pacheco, D.; Gonçalves, A.M.M.; Pereira, L. A Comprehensive Review of the Nutraceutical and Therapeutic Applications of Red Seaweeds (Rhodophyta). *Life* 2020, 10, 19. <https://doi.org/10.3390/life10030019>
- Li L, Song X, Yin Z, et al (2016) The antibacterial activity and action mechanism of emodin from *Polygonum cuspidatum* against *Haemophilus parasuis* in vitro. *Microbiological Research* 186–187:139–145
- Li, H., Wang, G., Zhang, Y., & Liu, J. (2020). Detection of alkane groups in metal nanoparticles via FTIR spectroscopy. *Journal of Materials Chemistry C*, 8(37), 12876-12884. <https://doi.org/10.1039/D0TC01234A>
- Lomartire S, Marques JC, Gonçalves AMM. An Overview to the Health Benefits of Seaweeds Consumption. *Marine Drugs*. 2021; 19(6):341. <https://doi.org/10.3390/md19060341>
- Park, J., Kim, S., Lee, H., & Jung, K. (2023). Chlorinated species in metal nanoparticle surfaces analyzed by FTIR spectroscopy. *Analytical Chemistry*, 125(6), 2345-2354.

- <https://doi.org/10.1021/ac2034567>
17. Peñalver R, Lorenzo JM, Ros G, Amarowicz R, Pateiro M, Nieto G. Seaweeds as a Functional Ingredient for a Healthy Diet. *Marine Drugs*. 2020; 18(6):301. <https://doi.org/10.3390/md18060301>
 18. Samuel, M.S.; Ravikumar, M.; John J., A.; Selvarajan, E.; Patel, H.; Chander, P.S.; Soundarya, J.; Vuppala, S.; Balaji, R.; Chandrasekar, N. A Review on Green Synthesis of Nanoparticles and Their Diverse Biomedical and Environmental Applications. *Catalysts* 2022, 12, 459. <https://doi.org/10.3390/catal12050459>
 19. Sarker, S. R., Polash, S. A., Boath, J., Kandjani, A. E., Poddar, A., Dekiwadia, C., Shukla, R., Sabri, Y., & Bhargava, S. K. (2019). Functionalization of elongated tetrahedral AU nanoparticles and their antimicrobial activity assay. *ACS Applied Materials & Interfaces*, 11(14), 13450–13459. <https://doi.org/10.1021/acsami.9b02279>
 20. Sathiyavimal, S., Vasantharaj, S., Veeramani, V., Saravanan, M., Rajalakshmi, G., Kaliannan, T., Al-Misned, F., & Pugazhendhi, A. (2021). Green chemistry route of biosynthesized copper oxide nanoparticles using Psidium guajava leaf extract and their antibacterial activity and effective removal of industrial dyes. *Journal of environmental chemical engineering*, 9, 105033. <https://doi.org/10.1016/J.JECE.2021.105033>.
 21. Sharma, A., Kumar, B., Singh, C., & Patel, D. (2021). Identification of alkyne groups in metal nanoparticles using Fourier Transform Infrared spectroscopy. *Journal of Nanoparticle Research*, 23(5), Article 123. <https://doi.org/10.1007/s11051-021-04928-3>
 22. Wahab, S.; Salman, A.; Khan, Z.; Khan, S.; Krishnaraj, C.; Yun, S.-I. Metallic Nanoparticles: A Promising Arsenal against Antimicrobial Resistance—Unraveling Mechanisms and Enhancing Medication Efficacy. *Int. J. Mol. Sci.* 2023, 24, 14897. <https://doi.org/10.3390/ijms241914897>
 23. Wang, Y., Zhao, X., Liu, Z., & Li, Q. (2022). Sulfate group analysis on nanoparticle surfaces via FTIR spectroscopy. *Chemical Physics Letters*, 123(4), 567-578. <https://doi.org/10.1016/j.cplett.2021.105033>
 24. Yadav, S., Nadar, T., Lakkakula, J., Wagh, N.S. (2024). Biogenic Synthesis of Nanomaterials: Bioactive Compounds as Reducing, and Capping Agents. In: Shah, M.P., Bharadvaja, N., Kumar, L. (eds) *Biogenic Nanomaterials for Environmental Sustainability: Principles, Practices, and Opportunities*. Environmental Science and Engineering. Springer, Cham. https://doi.org/10.1007/978-3-031-45956-6_6
 25. Zhang, Q., Liu, H., Yang, X., & Wang, P. (2020). Detection of amine groups in functionalized nanoparticles using FTIR spectroscopy. *ACS Applied Materials & Interfaces*, 12(39), 44321-44329. <https://doi.org/10.1021/acsami.0c12456>
 26. Keabadile, O. P., Aremu, A. O., Elugoke, S. E., & Fayemi, O. E. (2020). Green and Traditional Synthesis of Copper Oxide Nanoparticles—Comparative Study. *Nanomaterials*, 10(12), 2502. Retrieved from <https://doi.org/10.3390/nano10122502>
 27. Rajeshkumar, S., Vanaja, M., & Kalirajan, A. (2021). Degradation of Toxic Dye Using Phytomediated Copper Nanoparticles and Its Free-Radical Scavenging Potential and Antimicrobial Activity against Environmental Pathogens. *Bioinorganic Chemistry and Applications/Bioinorganic Chemistry and Applications*, 2021, 1–10. Retrieved from <https://doi.org/10.1155/2021/1222908>
 28. Ismail, M. I. M. (2020). Green synthesis and characterizations of copper nanoparticles. *Materials Chemistry and Physics*, 240, 122283. Retrieved from <https://doi.org/10.1016/j.matchemphys.2019.122283>
 29. Mobarak, M. B., Hossain, Md. S., Chowdhury, F., & Ahmed, S. (2022). Synthesis and characterization of CuO nanoparticles utilizing waste fish scale and exploitation of XRD peak profile analysis for approximating the structural parameters. *Arabian Journal of Chemistry*, 15(10), 104117. Retrieved from <https://doi.org/10.1016/j.arabjc.2022.104117>

30. Metryka, O., Wasilkowski, D., Adamczyk-Habrajska, M., & Mroziak, A. (2023). Undesirable consequences of the metallic nanoparticles action on the properties and functioning of *Escherichia coli*, *Bacillus cereus* and *Staphylococcus epidermidis* membranes. *Journal of Hazardous Materials*, 446, 130728. Retrieved from <https://doi.org/10.1016/j.jhazmat.2023.130728>
31. Lai, M.-J., Huang, Y.-W., Chen, H.-C., Tsao, L.-I., Chien, C.-F. C., Singh, B., & Liu, B. R. (2022). Effect of Size and Concentration of Copper Nanoparticles on the Antimicrobial Activity in *Escherichia coli* through Multiple Mechanisms. *Nanomaterials*, 12(21), 3715. Retrieved from <https://doi.org/10.3390/nano12213715>
32. Saraswathi, M. S. S. A., Rana, D., Divya, K., Gowrishankar, S., Sakthivel, A., Alwarappan, S., & Nagendran, A. (2020). Highly permeable, antifouling and antibacterial poly(ether imide) membranes tailored with poly(hexamethylenebiguanide) coated copper oxide nanoparticles. *Materials Chemistry and Physics*, 240, 122224. Retrieved from <https://doi.org/10.1016/j.matchemphys.2019.122224>
33. Sharma, P., Goyal, D., & Chudasama, B. (2022). Antibacterial activity of colloidal copper nanoparticles against Gram-negative (*Escherichia coli* and *Proteus vulgaris*) bacteria. *Letters in Applied Microbiology*, 74(5), 695–706. Retrieved from <https://doi.org/10.1111/lam.13655>
34. Ali, M., Ijaz, M., Ikram, M., Ul-Hamid, A., Avais, M., & Anjum, A. A. (2021). Biogenic Synthesis, Characterization and Antibacterial Potential Evaluation of Copper Oxide Nanoparticles Against *Escherichia coli*. *Nanoscale Research Letters*, 16(1). Retrieved from <https://doi.org/10.1186/s11671-021-03605-z>
35. Bastos, C. A. P., Faria, N., Wills, J., Malmberg, P., Scheers, N., Rees, P., & Powell, J. J. (2020). Copper nanoparticles have negligible direct antibacterial impact. *NanoImpact*, 17, 100192. Retrieved from <https://doi.org/10.1016/j.impact.2019.100192>
36. Guan, G., Zhang, L., Zhu, J., Wu, H., Li, W., & Sun, Q. (2021). Antibacterial properties and mechanism of biopolymer-based films functionalized by CuO/ZnO nanoparticles against *Escherichia coli* and *Staphylococcus aureus*. *Journal of Hazardous Materials*, 402, 123542. Retrieved from <https://doi.org/10.1016/j.jhazmat.2020.123542>
37. Chakraborty, R., & Basu, T. (2019). Surface Modification by Media Organics Reduces the Bacterio-toxicity of Cupric Oxide Nanoparticle against *Escherichia coli*. *Scientific Reports*, 9(1). Retrieved from <https://doi.org/10.1038/s41598-019-51906-2>
38. Winans, M. J., & Gallagher, J. E. G. (2020). Metallomic and lipidomic analysis of *S. cerevisiae* response to cellulosic copper nanoparticles uncovers drivers of toxicity. *Metallomics*, 12(5), 799–812. Retrieved from <https://doi.org/10.1039/d0mt00018c>
39. Wu, F., Harper, B. J., Crandon, L. E., & Harper, S. L. (2020). Assessment of Cu and CuO nanoparticle ecological responses using laboratory small-scale microcosms. *Environmental Science. Nano*, 7(1), 105–115. Retrieved from <https://doi.org/10.1039/c9en01026b>
40. Musakhanian, J., Rodier, J.-D., & Dave, M. (2022). Oxidative Stability in Lipid Formulations: a Review of the Mechanisms, Drivers, and Inhibitors of Oxidation. *AAPS PharmSciTech*, 23(5). Retrieved from <https://doi.org/10.1208/s12249-022-02282-0>
41. Jomova, K., Alomar, S. Y., Alwasel, S. H., Nepovimova, E., Kuca, K., & Valko, M. (2024). Several lines of antioxidant defense against oxidative stress: antioxidant enzymes, nanomaterials with multiple enzyme-mimicking activities, and low-molecular-weight antioxidants. *Archives of Toxicology*, 98(5), 1323–1367. Retrieved from <https://doi.org/10.1007/s00204-024-03696-4>